Experimental investigation on a Common Rail Diesel engine partially fuelled by Syngas

Carlo Alberto Rinaldini[a,*], Giulio Allesina[a], Simone Pedrazzi[a], Enrico Mattarelli[a], Tommaso Savioli[a], Nicolò Morselli[a], Marco Puglia[a], Paolo Tartarini[a]

[a] University of Modena and Reggio Emilia, Department of Engineering 'Enzo Ferrari',

Via Vivarelli 10/1, 41125 Modena, Italy

[*] Corresponding author, email address: carloalberto.rinaldini@unimore.it

Abstract

The high efficiency, reliability and flexibility of modern passenger car Diesel engines makes these power units quite attractive for steady power plants totally or partially running on fuels derived from biomass, in particular on syngas. The engine cost, which is obviously higher than that of current industrial engines, may not be a big obstacle, provided that the re-engineering work is limited and that performance and efficiency are enhanced. The goal of this work is to explore the potential of a current automotive turbocharged Diesel engine running on both Diesel fuel and syngas, by means of a comprehensive experimental investigation focused on the combustion process. The engine is operated at the most typical speed employed in steady power plants (3000 rpm), considering three different loads (50-100-300 Nm / 16-31-94 kW). For each operating condition, the syngas rate is progressively increased until it provides a maximum heating power of 85 kW, while contemporarily reducing the amount of injected Diesel oil. Maximum care is applied to guarantee a constant quality of the syngas flow throughout the tests, as well as to maintain the same engine control parameters, in particular the boost pressure.

It is found that in-cylinder pressure traces do not change very much, even when drastically reducing the amount of Diesel fuel: this is a very encouraging result, because it demonstrates that there is no need to radically modify the standard stock engine design. Another promising outcome is the slight but consistent enhancement of the engine brake efficiency: the use of syngas not only reduces the consumption of Diesel oil, but it also improves the combustion quality.

The authors acknowledge that this study is only a starting basis: further investigation is required to cover all the aspects related to the industrial application of this syngas-Diesel combustion concept, in particular the impact on pollutant emission and on engine durability.

Keywords: Dual-Fuel, syngas, Diesel, combustion, engine

Nomenclature

C	flow coefficient [-]
CAD	crank angle degrees
LHV_{CO}	CO lower heating value [MJ/ Nm^3]
LHV_{CH_4}	CH_4 lower heating value [MJ/ Nm^3]
LHV_{Diesel}	Diesel oil lower heating value [MJ/kg]
LHV_{H_2}	H_2 lower heating value [MJ/ Nm^3]
LHV_{syngas}	syngas lower heating value [MJ/Nm^3]
MFB	mass fraction burnt
Q	syngas volumetric flow rate [m^3/s]
$Q_{N,syngas}$	syngas volumetric flow rate at standard ambient conditions (0 °C and 101325 Pa) [Nm^3/s]
P_{syngas}	syngas heating power [kW]
P	engine brake power [kW]
d	nominal diameter of the orifice [m^2]
$\dot{m}_{Diesel}$	Diesel oil mass flow rate [kg/s]
x_{H_2}	H_2 molar fraction in syngas composition
x_{CO}	CO molar fraction in syngas composition
x_{CH_4}	CH_4 molar fraction in syngas composition
x_{syngas}[%]	potential energy provided by syngas [%]

Greeks

β	ratio of the orifice diameter to the pipe diameter [-]
ε	compressibility coefficient [-]
η_b	engine brake efficiency [-]
ρ_1	gas density upstream the orifice [kg/m^3]
Δp	pressure drop across the orifice [Pa]

Subscript

DF	Dual Fuel operation
ND	Normal Diesel operation

Acronyms

CI	Compression Ignition
ECU	Electronic Control Unit
EGR	Exhaust Gas Recirculation
HSDI	High Speed Direct Injection
SI	Spark Ignition
UEGO	Universal Exhaust Gas Oxygen
VGT	Variable Geometry Turbocharger

1 Introduction

The share of renewable energy resources in the energy mix is increasing every year, pushed by economical and sustainability drivers. The shortage and the unpredictability of the conventional energy sources afflicted by depletion and global geo-political issues are causing an energy crisis that is accelerating the renewable energy climb [1,2]. The so called renewables promise clean energy production from sources such as the sun, wind, water and biomass. The transition to sustainability is slowed down by the discontinuity in the energy production from such sources. In particular, solar power and wind power are not always available when needed [3,4]. This is a well-known issue that becomes quite critical in the case of off-grid applications, where nothing can compensate for a lowering or a stop in the energy production, leading to the impossibility to run electrical devices [2,3]. Conversely, biomass is a resource that, if properly managed, can be collected and used to produce power, independent from the environmental conditions. Its abundance makes it particularly attractive for power and heat generation [5,6,7].

Obviously, the technologies used to convert biomass into energy are not immune to power-on-demand related issues. Large biomass power plants, exploiting the Rankine steam cycle, are characterized by long warm-up periods and low flexibility in the amount of produced power. This aspect makes these systems unattractive for remote power production, but extremely interesting for transition from fossil fuels to large-scale power plants [7]. A promising alternative is the combined use of internal combustion-engine-based power plants and technologies able to convert the biomass into a suitable fuel [8-11].

The use of internal combustion engines, instead of turbines and steam generators, yields a number of advantages: first, the wide range of power ratings available in the market (from a few kWs to MWs); second, the capability of running on many different types of fuel; third, the fast and reliable control of the power output; fourth, the high level of technical sophistication, achieved through more than a century of continuous research and development worldwide in the automotive and industrial field. Last but not least, the widespread know-how on internal combustion engines greatly simplifies the issues related to the system management and maintenance [8,9,12].

Due to the advantages listed above, both Spark Ignition (SI) and Compression Ignition (CI) engines are widely used in renewable energy systems: SI engines can run on natural gas, ethanol, hydrogen, and biogas, while compression ignition is applied to burn any type of vegetable oil, waste-derived oil and biodiesel [13-18]. Literature shows also examples of dual fuel applications on CI engines, combining gaseous fuels and diesel oil or vegetable oil [6,19].

In the case of biomass gasification, the produced gaseous fuel, known as syngas, is composed mainly of hydrogen, carbon monoxide, carbon dioxide, nitrogen and methane [20]. The properties of this gas allow a standard SI engine to be easily converted from gasoline to syngas, at the cost of a reduction of the maximum brake power output [20-22]. The conversion consists of two main parts: first, it is necessary to modify the engine intake manifold in order to mix syngas and air; second, a new throttle valve must be installed for controlling the airflow rate, so that the air-syngas mixture within the cylinders is about stoichiometric. This control is enabled by a Lambda sensor (UEGO sensor) installed in the exhaust manifold, and by a dedicated electronic control unit [22].

Syngas may also be used in CI engines, and this option is very attractive for many reasons: first, Diesel engines are more widespread than SI engines as off-road and industrial power plants, due to their robustness and fuel efficiency; second, only minor hardware modifications are required to run on dual fuel mode (no need of a spark plug, since a small amount of Diesel fuel can be employed to ignite the air-syngas mixture [5,23]). The combination of syngas and Diesel is an improvement compared to both conventional SI and CI engines: in comparison with a SI engine converted to run on syngas, brake efficiency is higher, due to the higher compression ratio and the lower pumping losses (load can be controlled without throttling); in comparison with a standard Diesel engine, considering a constant load, the replacement of diesel fuel with

syngas is highly beneficial for soot emissions [5]. The fact that a CI engine cannot be operated without at least a small amount of Diesel fuel is a minor limitation: it just implies the necessity of a fuel tank close to the engine. Finally it should also be considered that the power rating of a Diesel engine converted to syngas is much less penalized than in the case of conversion from a gasoline engine [24-26].

The cases described in literature often refer to tests carried out on small single-cylinder Diesel engines [23,27]. In the authors' knowledge, the technical literature lacks studies referring to engines characterized by high power ratings and electronically controlled injection systems, as typically found in passenger cars. It is easy to predict that this type of engines will become of great interest for stationary power plants, in view of their decreasing costs (the technology has already been developed in the automotive field, while the production costs are abated by the availability of existing plants). The main advantage provided by the use of Diesel engines derived from the automotive industry consists in the high number of control parameters, thus a superior capability to optimize unconventional engine operations [8]. On the other hand, however, these engines require a huge calibration work, to exploit their full potential, as well as to prevent failures due to the unconventional use.

This work is aimed at describing the effects of syngas-diesel oil combustion in a recent automotive 4-stroke, 4-cylinder, 2.7 litre, turbocharged Diesel engine, equipped with a 160 MPa Common Rail injection system and a high pressure EGR circuit**.** Tests with different syngas Diesel oil ratios are performed at 3000 rpm, in order to produce results comparable with other engines used for power generation at 50 Hz.

The facility used in this work is an air-blown downdraft gasifier fed with soft wood chip. The choice of a downdraft gasifier is due to the low tar and particulate content when compared to other gasification technologies [20,22]. This feature is related to the internal design of the downdraft gasifier, where tar produced in the pyrolysis stage is thermally converted into gas when passing through the combustion stage of gasification [20]. Even under these conditions, the tar amount of the producer gas in the downdraft gasifier is about 1 g/Nm^3 [20], too high for the application as fuel into an internal combustion engine. Basu and Knoef suggest that 0.1 g/Nm^3 is the maximum tar limit [20,22], therefore filtration remains a fundamental stage of these gasification systems [28]. In this work, the gasifier employs a batch packed-bed bio-filter to control the tar amount of the delivered gas.

2 Materials and methods

2.1 Gasifier

A description of the gasifier facility has already been provided in a previous paper [25], therefore, only the fundamentals will be reviewed here. A mix of poplar and pine wood chips with about 20 % of moisture is used as fuel. The biomass is converted into syngas in a downdraft single throat Imbert-type reactor. This system, when fuelled with high quality wood biomasses yields a gas whit a low tar content, suitable for engine applications [10, 11, 20]. The air needed for the gasification reaction is pumped into the reactor by a blower. The produced gas is filtered in a double cyclone in order to separate particles from the gas stream. The resulting syngas is finally cooled and filtered in a drum filter filled with soft wood chips. At the top of the filter, a foam disk prevents wood dust and other fine particles to be carried out by the syngas stream. This type of filter, described by Allesina et al. [28], is proven to be suitable to match the requirements of a modern internal combustion engine, being able to effectively purge water and tar from the syngas [29].

The gasifier is designed to produce a maximum flow rate of 60 Nm^3/h, corresponding to a heating power of about 85 kW. After filtration, the syngas is pumped to the engine facility depicted in Figure 1. During the test, some syngas is continuously spilled and analysed by a Pollution micro gas chromatographer (device 16, Figure 2), in order to assess the average syngas composition. The gas flow rate is measured according to the

UNI EN ISO 5167 standard [30], using a calibrated orifice, equipped with a differential pressure manometer and a thermocouple for syngas temperature measurement (device 15, Figure 2). The volumetric flow rate of the syngas, is calculated according to the following equation:

$$Q = \frac{C}{\sqrt{1-\beta^4}} \varepsilon \frac{\pi d^2}{4} \sqrt{2\rho_1 \Delta p} \tag{1}$$

where:

Q is the volumetric flow rate;

β is the ratio of the orifice diameter to the pipe diameter;

C is the flow coefficient calculated as function of β and of the Reynolds number, according to [30];

d is the nominal diameter of the orifice (38.1 mm);

ρ_1 is the gas density upstream of the orifice;

Δp is the pressure drop across the orifice measured by the manometer;

ε is the compressibility coefficient calculated as function of β, the pressure upstream of the orifice, the syngas politropic coefficient and Δp.

The temperature upstream of the orifice is measured by a K-type thermocouple.

To assess the syngas heating power (potential chemical energy) provided to the engine, the following equations are applied:

$$P_{syngas} = 10^3 \cdot LHV_{syngas} \cdot Q_{N,syngas} \tag{2}$$

$$LHV_{syngas} = LHV_{H_2} \cdot x_{H_2} + LHV_{CO} \cdot x_{CO} + LHV_{CH_4} \cdot x_{CH_4} \tag{3}$$

where:

P_{syngas} is the syngas heating power in kW;

LHV_{syngas} is the syngas lower heating value in MJ/Nm^3 calculated by Eq. 3;

$Q_{N,syngas}$ is the syngas flow rate in Nm^3/h at standard ambient conditions (0 °C and 101325 Pa) calculated using perfect gas law;

LHV_{H_2}, LHV_{CO} and LHV_{CH_4} are the lower heating value in MJ/Nm^3 of H_2, CO and CH_4 extracted from [31];

x_{H_2}, x_{CO} and x_{CH_4} are the molar fraction of H_2, CO and CH_4 in the syngas.;

2.2 Engine and experimental setup

The engine employed in the test is a current passenger car 2.8 litre turbocharged Diesel engine, of which, the main characteristics are shown in Table 1. During the test, the engine control unit is connected to an ETAS calibration interface and the ETAS INCA software is used to check and manage the operating parameters.

The experiments are performed at the University of Modena and Reggio Emilia engine test bed (Figure 1), featuring an Apicom FR 400 BRV eddy-current brake and the Apicom Horus software for system control and data acquisition. Besides the standard pressure and temperature transducers, the laboratory instruments also include a Coriolis flow meter for measuring the Diesel fuel consumption. A high frequency specifically designed indicating system is installed in order to record in-cylinder pressure traces; the system is made up of a Kistler piezoelectric transducer, installed on cylinder #1 in place of the glow plug, a charge amplifier

and an optical encoder. A time-base method is used to acquire in-cylinder pressure traces while the real time calculation is performed by the Alma Automotive software on the National Instruments Compact RIO hardware. The resulting angular resolution is 0.3°. A sketch of the experimental setup, including some further details, is shown in Figure 2.

Table 1 Engine main data

Engine type	HSDI 4-S diesel
Manufacturer	VM Motori
Model	RA 428
Number of cylinder	4 in-line
Total displacement (cm3)	2776
Bore x Stroke (mm)	94 x 100
Compression ratio	17.5:1
# of valves per cylinder	4
Air metering	VGT, Intercooler
Injection system	Common rail
Max. injection press (MPa)	160
Max Power	130 kW@3800 rpm

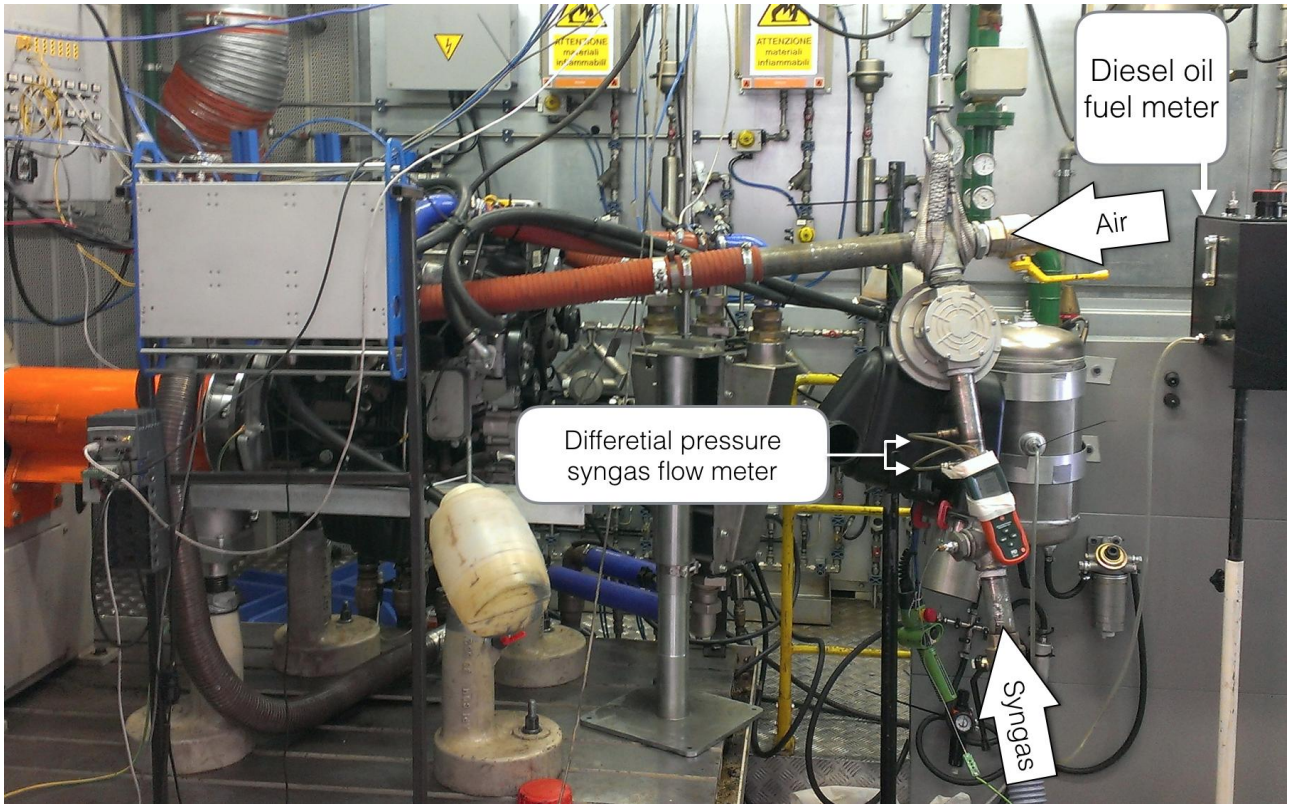

Figure 1 *The VM engine at the test bench*

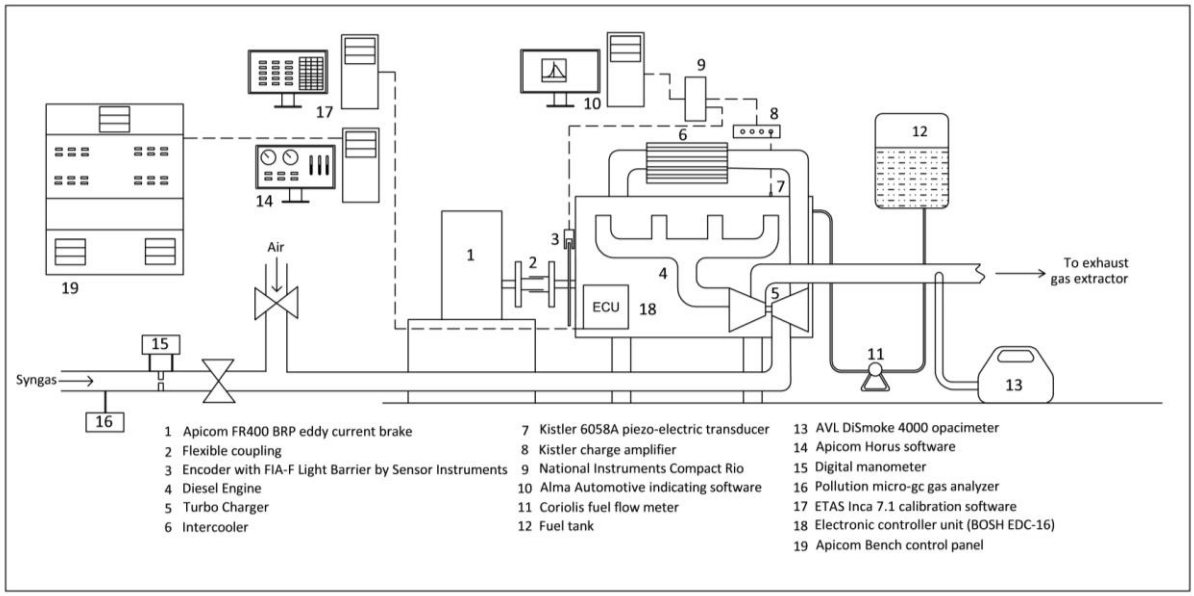

Figure 2 *Sketch of the experimental setup*

2.3 Conduct of experiments

The test procedure consists of running the engine at 3000 rpm and 3 different engine outputs (brake torque: 50, 100 and 300 Nm), reproducing the most typical conditions occurring when the engine is coupled to a 50 Hz electric generator. During the tests, 2 closed-loop controls are used: the former is applied to the eddy-current brake in order to control the rotational speed, the latter is applied to the engine pedal in order to control the output torque. For each operating point, the tests always starts running the engine on Diesel oil (this operating point is referred to as ND, Normal Diesel); then, the amount of syngas is progressively increased, recording engine performance for each Dual Fuel (DF) steady operating point. Finally, the ND operating point is repeated, in order to check the engine conditions, and to guarantee the repeatability of the measures. As the syngas flow rate increases, the closed loop engine control automatically adjusts the engine pedal in order to keep the torque on the target value. It is important to remark that the pedal position in automotive engines is a paramount input for most ECU maps: besides the amount of injected fuel, a pedal variation may affect the boost pressure, the injection strategy and the EGR rate. Maximum care is applied to maintain the operating conditions as close as possible, when varying the syngas rate. This is the reason why

the EGR valve is blocked, and the boost pressure is controlled by the ETAS software. As an example of what happens when boost pressure is not controlled, Figure 3 shows in-cylinder pressure traces for a load of 100 Nm, running on ND, and two different syngas rates (2 larger than 1). As the syngas rate increases, the pedal rate decreases; both injected fuel and boost pressure are lower, then the mass of the charge trapped within the cylinder goes down, as demonstrated by the lower pressure values throughout compression. In this condition, combustion efficiency may drop abruptly due to the lack of oxygen, defeating all the benefits provided by the syngas use. Fortunately, in modern Diesel engines the problem may be avoided controlling the turbocharger: in this case, the turbine rack can be adjusted and the boost pressure can be kept constant for a wide range of syngas rates.

All the standard protocols for keeping the testing conditions as uniform as possible are followed: in particular, the temperature of: Diesel fuel, syngas, engine lubrication oil and coolant is kept within a narrow range for all the cases. Moreover, the DF operating points are recorded when both increasing and decreasing the syngas rate, in order to eliminate any potential hysteresis effect.

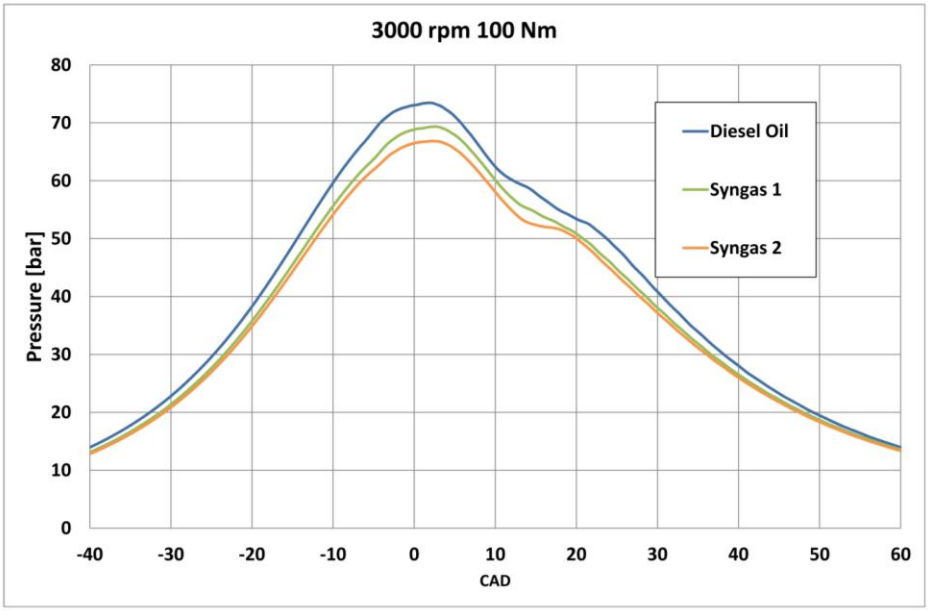

Figure 3 *In-cylinder pressure for different syngas level without modification on the engine boost pressure (Syngas 1 corresponds to 15% of Diesel oil substitution, Syngas 2 to 34%)*

3 Results

3.1 Gasifier

In order to speed up the warming process and to stabilize the gasifier conditions, the syngas produced by the gasifier is burned in a torch for about 1 hour. Only when the temperature of the reactor goes over 800 °C in the combustion zone, and 700 °C in the end of the reduction zone, the gasification occurs efficiently and it is possible to consider the gas quality good enough for internal combustion engine applications. Once these conditions are reached, the filtered syngas is delivered to the engine mixing system, monitoring the composition by a micro-GC. The average syngas composition and its lower heating value are shown in Table 2 while Table 3 reports the main physic-chemical properties of both syngas and Diesel oil. The values appear to be quite consistent with literature [20,22]. The higher heating value of the syngas is about 5 MJ/Nm^3, thus the maximum syngas heating power is about 82.5 kW. Considering a top engine efficiency of about 30%, the maximum syngas brake power substitution is 25 kW. The syngas amount is controlled by means of a ball

valve downstream of the calibrated orifice, as well as by throttling the gasifier air intake with another ball valve. Reactor temperature and syngas composition are kept stable during the test. In order to avoid the saturation of the drum filter capacity, with an ensuing worsening of the syngas quality, the test is stopped after about 3 hours. The filter condition is inspected after the test. In the experiments carried out in this study, condensates were never detected in the foam at the top of the wood chip bed, demonstrating the good working condition of the filter. However, the hydrogen content in the gas resulted lower when compared to other tests ran at the same facility. In fact, reference [25] reports a series of tests where the H_2 content never went below 19 % while CH_4 never exceeded 1.8 %. The reasons behind this performance reduction are not investigated in this work. Nevertheless the following hypotheses are made:

- The tests performed in this work are characterized by a series of pulses in the syngas flow rate drawn from the gasifier. Literature suggest that, for unsteady operating conditions, a double throat design is more suitable than the single throat one [32].
- Sudden pressure drops in the gasifier-filter system were observed when the engine moved from low to high loads: these pressure drops may have violated the one-of-a-kind requirement of the filtration system described in [25]. As a result, part of the "head" gas from the reactor may have leaked into the filtration system and mixed with the downdraft gas.

Table 2 Syngas composition and calculated Lower Heating Value

	H_2 [%mol.]	N_2 [%mol.]	CO [%mol.]	CO_2 [%mol.]	CH_4 [%mol.]	H_2O [%mol.]	LHV [MJ/Nm^3]
Wet gas	*8.7*	*54.7*	*20.6*	*5.0*	*3.1*	*7.9*	*4.54*
Dry gas	*9.4*	*59.4*	*22.4*	*5.4*	*3.4*	*0*	*5.07*

Table 3 *Comparative physic-chemical characterization of diesel oil and syngas*

	Syngas (dry)	**Diesel oil (EN 590:1999) [15]**
State at 20 °C	*Gas*	*Liquid*
Density at 20 °C	*1.09 kg/m3*	*838 kg/m3*
Cinematic viscosity	*15 mm²/s [33]*	*2-4.5 mm²/s*
LHV	*4.65 MJ/kg*	*42.5 MJ/kg*

3.2 Engine outputs

As already mentioned, experimental tests are carried out running the engine on standard Diesel (ND) and Dual Fuel diesel/syngas (DF), at about 30 steady state operating points, one engine speed (3000 rpm). Each operating point is defined by its brake torque (50-100-300 Nm) and by the fuel composition, expressed as the fraction of potential energy provided by Syngas:

$$Xsyngas[\%] = \frac{P_{syngas} + LHV_{Diesel} \cdot \dot{m}_{Diesel,DF}}{LHV_{Diesel} \cdot \dot{m}_{Diesel,ND}} \cdot 100 \tag{4}$$

where LHV stands for lower heating value, $\dot{m}$ is the mass flow rate.

The lower heating value of the syngas is calculated from its composition, measured during the test using the gas chromatography system. The maximum syngas energy substitution rate is limited by the gasifier production rate, which is low in comparison to the engine maximum power output: therefore, the maximum percentage of syngas (60%) can be reached only at 50 Nm.

Figure 4 shows the normalized consumption of the engine in terms of Diesel fuel, as a function of the syngas rate (normalization performed by dividing the current fuel rate by the one measured in ND condition). The map reported in Figure 5, presenting the engine brake efficiency as a function of brake torque and syngas rate, is constructed interpolating by triangulation the whole set of tested operating points. To enhance the

interpretation of the diagram, some interpolation lines (calculated according to the ordinary least squares method) are added to Figure 4. The interpolation functions and the correlation coefficients are shown in the graph, whereas the values are reported in the Appendix, for the sake of brevity.

At 50 and 100 Nm it can be observed that the reduction of Diesel fuel perfectly corresponds to the increase of syngas rate: as an example, 30% of syngas reduces the amount of injected Diesel fuel by 30%. At 300 Nm, however, the engine appears more efficient when running on syngas. As an example, a 25% of Syngas enables a 30% reduction of Diesel fuel consumption. This outcome is confirmed by Figure 5, showing the engine brake efficiency (or global efficiency), defined as follows:

$$\eta_b = \frac{P}{P_{syngas} + LHV_{Diesel} \cdot \dot{m}_{Diesel,DF}} \cdot 100 \qquad (5)$$

The maximum improvement on the engine brake efficiency at 300 Nm is 10%, reached with a syngas energy substitution rate of about 27%. The maximum absolute values of brake efficiency are obviously obtained at the higher load (300 Nm), for the lower weight of mechanical friction losses. The higher sensitivity to syngas substitution at high loads, clearly visible in figure 4, can be expected too. Thermodynamic cycle efficiency is generally related to combustion velocity: the higher, the better, except when there is an abrupt increase of heat transfer. At high loads, combustion tends to have a larger angular duration, so the enhancement of combustion speed ensuing the syngas introduction has a stronger influence.

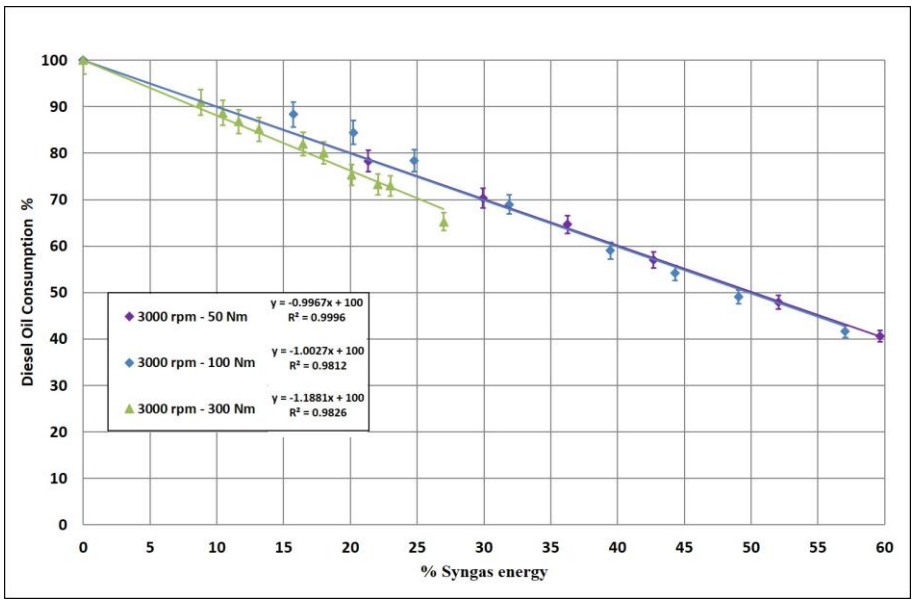

Figure 4 *Diesel oil consumption as a function of syngas potential energy for different engine loads*

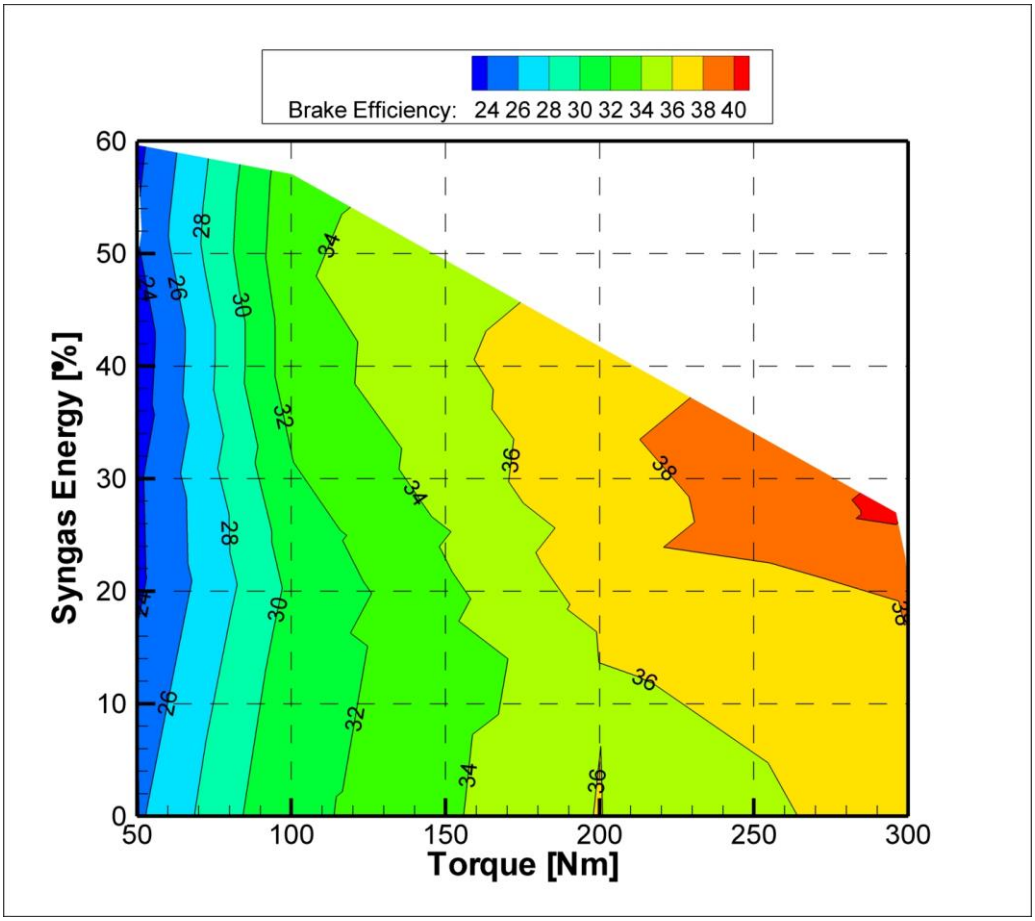

Figure 5 *Engine brake efficiency as a function of syngas potential energy and engine loads*

In order to gain a better insight on Dual Fuel combustion, as well as to provide an explanation to the improvement of brake efficiency shown in Figure 5, in-cylinder pressure traces are recorded for 100 consecutive cycles, at any operating condition. Figures 6, 7 and 8 show the most representative ensemble-averaged pressure traces, while Figures from 9 to 14 review the parameters typically employed to analyse combustion. In particular, the Rate of Heat Release (RoHR) for 50 Nm, 100 Nm and 300 Nm of torque is depicted in Figures 9, 10 and 11. The RoHR is defined as the net rate of energy (difference between the heat released by combustion and the heat rejected through the walls) provided to the charge and it is calculated according to the Rassweiler and Withrow method [34]. Angles at which 10, 50 and 90% of fuel is burnt are reported for the three values of torque in Figure 12. Finally, 0-10% and 10-90% combustion durations are plotted in Figures 13 and 14. All the numerical values of figures 12-14 are shown in the Appendix.

It should be observed that injection strategies change as load increases: while at 50 and 100 Nm there are three consecutive injections (pilot, pre and main), at 300 Nm the pilot injection is suppressed.

Looking at the in-cylinder pressure traces (Figures 6-8) and at the RoHR curves (Figures 9-11) the following considerations can be made:

- In the very first phase of combustion, the presence of syngas in the charge, seems to cause a slightly larger auto-ignition delay of the injected Diesel oil; as the syngas rate increases, this behaviour becomes much more evident. This outcome may be easily explained considering that, as the syngas rate increases, the oxygen concentration within the trapped charge is lower.
- After the start of combustion, all DF configurations present a higher RoHR, in comparison to ND combustion: this is the evidence that the syngas fuel within the trapped charge is ignited by the pilot and the pre injections. As a result, the first combustion development is quicker (see also 10% burnt angle in Figure 12, and 0-10% combustion angles in Figure 13), and in-cylinder pressure is always

higher for all DF configurations in the 0-15° after top dead centre interval. Considering that a faster combustion is generally associated with a more effective thermodynamic cycle, as well as with a more complete combustion, it may be inferred that the advantage of syngas, in terms of brake efficiency shown by Figure 5, is related to this aspect.

- From 15° after TDC, the combustion rate associated with syngas decreases, in comparison to ND, since the energy has already been released in the previous phase (see also the 10-90% combustion duration in figure 14). The differences fade away beyond 40° after TDC
- For all the investigated cases, combustion always starts after the first Diesel fuel injection, meaning that no auto-ignition occurs in the air-syngas mixture.
- Very small differences are observed on in-cylinder peak pressures, so that the mechanical reliability of the engine should not be affected.

In general, it is observed that even large rates of syngas have a limited effect on the pressure traces: this is the evidence that dual fuel combustion is a robust concept, and it may be safely applied to modern Diesel engines with a relatively limited amount of calibration and development work.

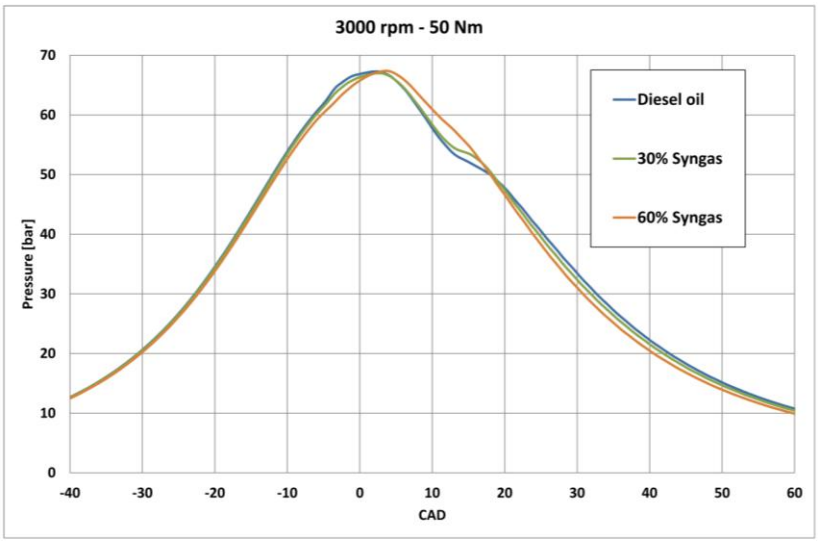

Figure 6 *In-cylinder pressure at 50Nm*

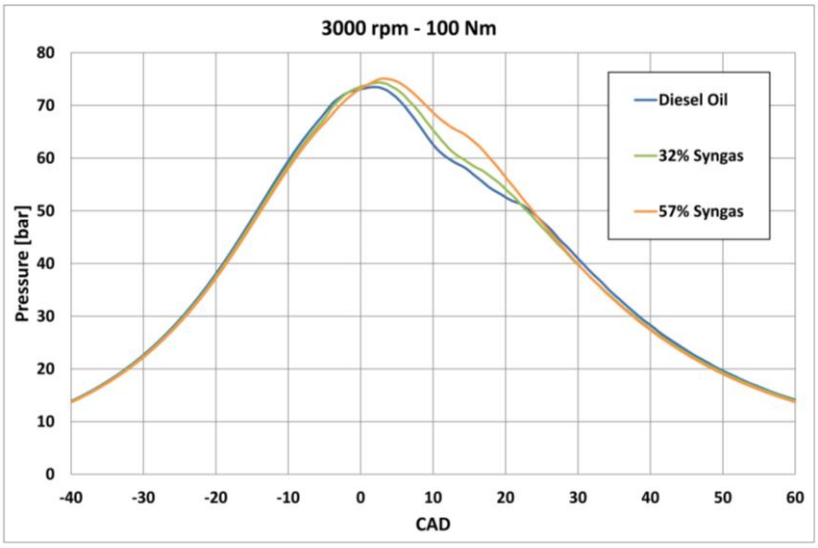

Figure 7 *In-cylinder pressure at 100Nm*

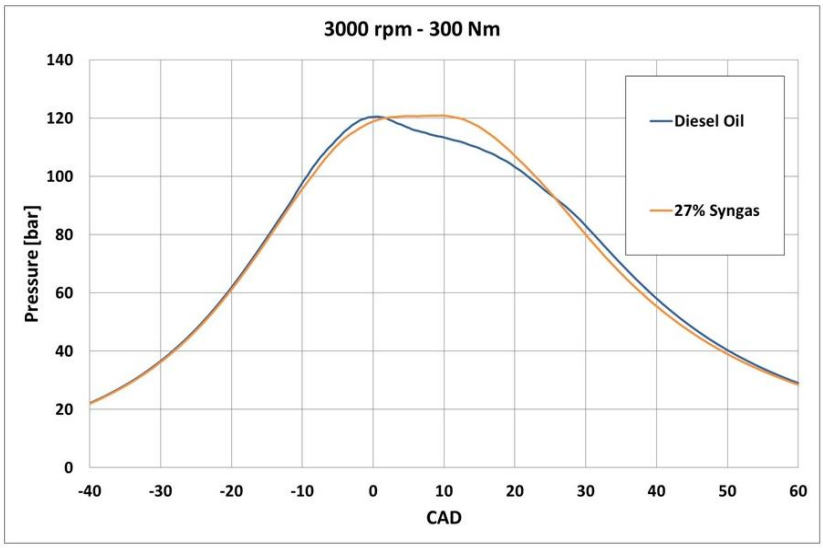

Figure 8 *In-cylinder pressure at 300Nm*

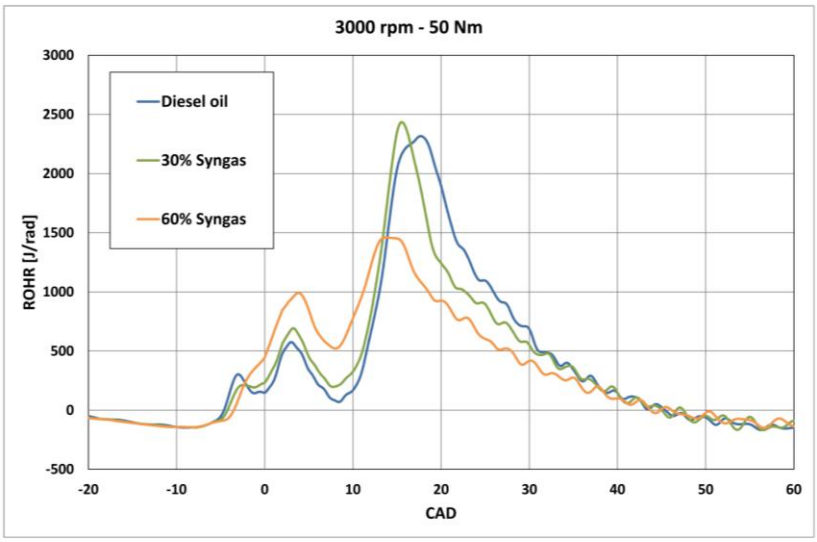

Figure 9 *Rate of Heat Release at 50Nm*

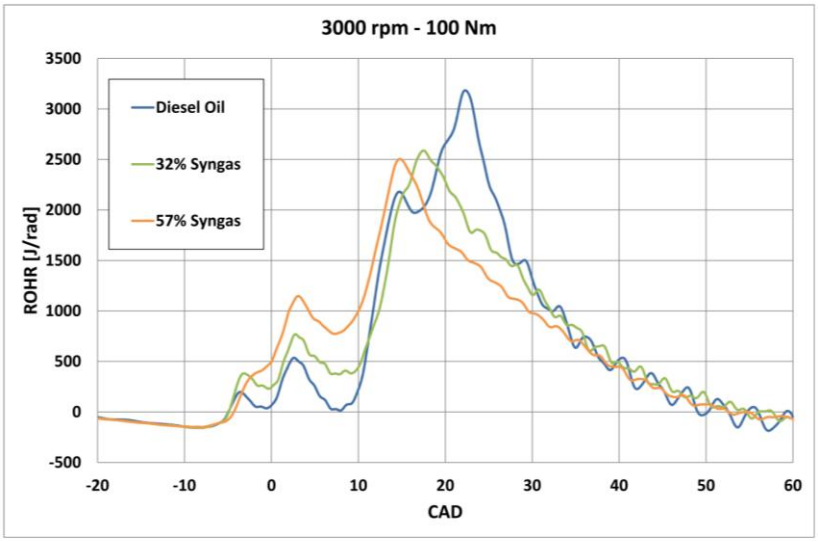

Figure 10 *Rate of Heat Release at 100Nm*

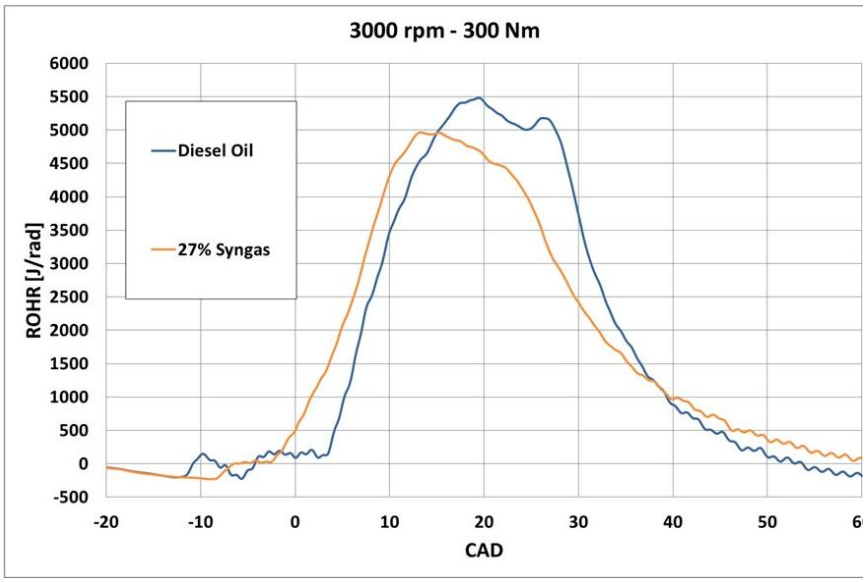

Figure 11 *Rate of Heat Release at 300Nm*

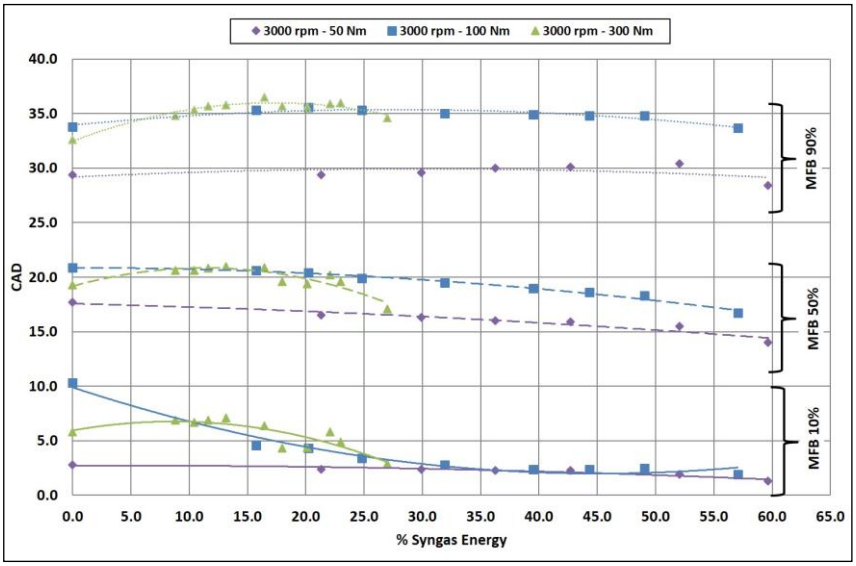

Figure 12 *Combustion angles for different syngas potential energy at 50 Nm, 100 Nm and 300 Nm*

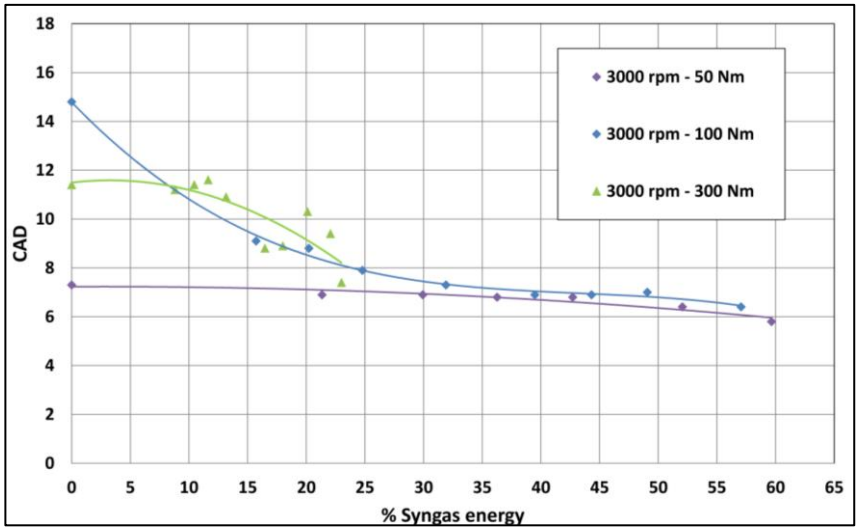

Figure 13 *Duration of the first part of the combustion process (0-10% MFB) for different syngas potential energy and different loads*

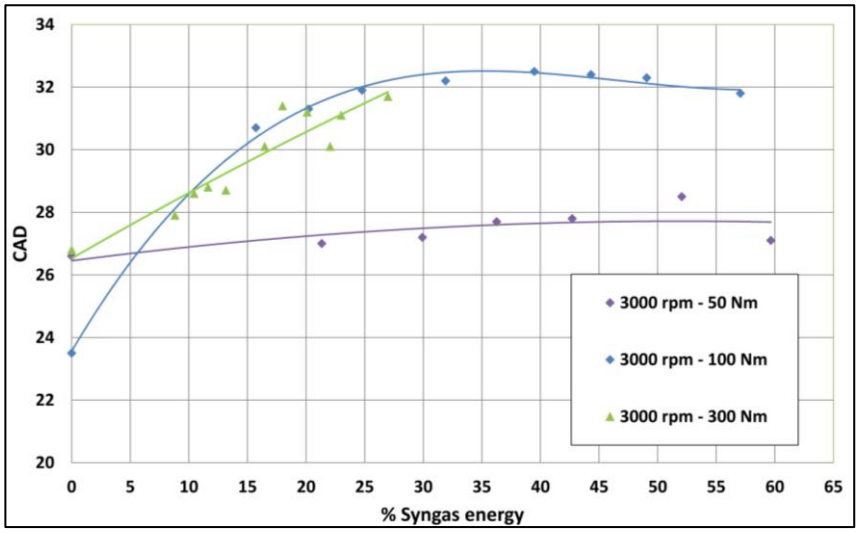

Figure 14 *Duration of the main part of the combustion process (10-90% MFB) for different syngas potential energy and different loads*

Conclusion

The goal of this work is to explore the potential of a current automotive turbocharged Diesel engine running on both Diesel fuel and syngas, by means of a comprehensive experimental investigation focused on the combustion process. The engine is operated at the typical speed employed in steady power plants (3000 rpm), considering three different loads (50-100-300 Nm / 16-31-94 kW). For each operating condition, the Syngas rate is progressively increased, while contemporarily reducing the amount of injected Diesel oil.

The syngas for the experiments is continuously provided by a gasifier connected to the engine. The higher heating value of the syngas is about 5 MJ/Nm^3, enabling a maximum syngas heating power of about 82.5 kW. A Diesel fuel substitution rate of about 60% is reached at 50 Nm. Particular care is also devoted to set the engine control parameters, such as boost pressure, injection advance, et cetera, in order to guarantee optimum combustion conditions, even with high rates of syngas.

It is found that the in-cylinder pressure traces do not change very much, even when drastically reducing the amount of Diesel fuel: this is a very encouraging result, because it demonstrates that there is no need to radically modify the standard stock engine design. Another promising outcome is the slight but consistent enhancement of the engine brake efficiency (up to +5%, with a 27% substitution rate). This increase is given by a faster combustion of the syngas-diesel fuel in comparison to normal diesel fuel. In conclusion, the use of syngas not only reduces the consumption of Diesel oil, but it also improves the combustion quality.

The authors emphasize that this study is only a starting basis: further investigation is required to cover all the aspects related to the industrial application of this syngas-Diesel combustion concept, in particular the impact on pollutant emissions and on engine durability.

References

1. Świątkiewicz-Mośny M, Wagner A, How much energy in energy policy? The media on energy problems in developing countries (with the example of Poland), Energy Policy, Volume 50, November 2012, Pages 383-390, ISSN 0301-4215, http://dx.doi.org/10.1016/j.enpol.2012.07.034.

2. Brandoni C, Arteconi A, Ciriachi G, Polonara F, Assessing the impact of micro-generation technologies on local sustainability, Energy Conversion and Management, Volume 87, November 2014, Pages 1281-1290, ISSN 0196-8904.

3. Fan Y, Mu A, Ma T, Study on the application of energy storage system in offshore wind turbine with hydraulic transmission, Energy Conversion and Management, Volume 110, 15 February 2016, Pages 338-346, ISSN 0196-8904, http://dx.doi.org/10.1016/j.enconman.2015.12.033.

4. El Fathi A, Nkhaili L, Bennouna A, Outzourhit A, Performance parameters of a standalone PV plant, Energy Conversion and Management, Volume 86, October 2014, Pages 490-495, ISSN 0196-8904, http://dx.doi.org/10.1016/j.enconman.2014.05.045.

5. Allesina G, Pedrazzi S, Rinaldini CA, Savioli T, Morselli N., Mattarelli E., Tartarini P Experimental-analytical evaluation of sustainable syngas biodiesel CHP systems based on oleaginous crop rotation (Conference Paper). International Conference on Power Engineering, ICOPE 2015; PACIFICO Yokohama Conference CenterYokohama; Japan; 30 November 2015 through 4 December 2015; Code 118770

6. Allesina G, Pedrazzi S, Rinaldini CA, Di Paola G, Morselli N, Savioli T, Mattarelli E, Tartarini P. Effect of syngas-CNG co-combustion on automotive engines for micro CHP applications. ASME-ATI- UIT 2015 Conference on Thermal Energy Systems: Production, Storage, Utilization and the Environment, 17 – 20 May, 2015, Napoli, Italy.

7. McKendry P, Energy production from biomass (part 2): conversion technologies, Bioresource Technology, Volume 83, Issue 1, May 2002, Pages 47-54, ISSN 0960-8524, http://dx.doi.org/10.1016/S0960-8524(01)00119-5.

8. Survey of modern power plants driven by diesel and gas engines - VTT www.vtt.fi/inf/pdf/tiedotteet/1997/T1860.pdf - S Niemi - 1997

9. Rinaldini C A, Mattarelli E, Savioli T, Cantore G, Garbero M., & Bologna A (2016). Performance, emission and combustion characteristics of a IDI engine running on waste plastic oil. Fuel, 183, 292-303.

10. Allesina G, Pedrazzi S, Tebianian S, Tartarini P Biodiesel and electrical power production through vegetable oil extraction and byproducts gasification: Modeling of the system (2014) Bioresource Technology, 170, pp. 278-285. DOI: 10.1016/j.biortech.2014.08.012

11. Pedrazzi S, Allesina G, and Tartarini P. Effects of upgrading systems on energy conversion efficiency of a gasifier - fuel cell - gas turbine power plant. Energy Conversion and Management, 126: 686 - 696, Ottobre 2016. http://dx.doi.org/10.1016/j.enconman.2016.08.048

12. Hossain AK, Davies PA, Plant oils as fuels for compression ignition engines: A technical review and life-cycle analysis, Renewable Energy, Volume 35, Issue 1, January 2010, Pages 1-13, ISSN 0960-1481, http://dx.doi.org/10.1016/j.renene.2009.05.009.

13. Homdoung N, Tippayawong N, Dussadee N, Performance and emissions of a modified small engine operated on producer gas, Energy Conversion and Management, Volume 94, April 2015, Pages 286-292, ISSN 0196-8904, http://dx.doi.org/10.1016/j.enconman.2015.01.078.

14. Henham A, Makkar MK Combustion of simulated biogas in a dual-fuel diesel engine, Energy Conversion and Management, Volume 39, Issues 16–18, November–December 1998, Pages 2001-2009, ISSN 0196-8904, http://dx.doi.org/10.1016/S0196-8904(98)00071-5.

15. Rinaldini C A, Mattarelli E, Magri M, & Beraldi M (2014). Experimental investigation on biodiesel from microalgae as fuel for diesel engines (No. 2014-01-1386). SAE Technical Paper.

16. Mattarelli E, Rinaldini CA, & Savioli T (2015). Combustion analysis of a diesel engine running on different biodiesel blends. Energies, 8(4), 3047-3057.

17. Mattarelli E, & Rinaldini C A (2015). Combustion Analysis on an IDI CI Engine Fueled by Microalgae (No. 2015-24-2484). SAE Technical Paper.

18. Bavutti M, Guidetti L, Allesina G, Libbra A, Muscio A, Pedrazz, S. Thermal stabilization of digesters of biogas plants by means of optimization of the surface radiative properties of the gasometer domes (2014) Energy Procedia, 45, pp. 1344- 1353. doi:10.1016/j.egypro.2014.01.141

19. Mattarelli E, Rinaldini C A, & Golovitchev V I (2014). CFD-3D analysis of a light duty Dual Fuel (Diesel/Natural Gas) combustion engine. Energy Procedia, 45, 929-937.

20. Basu P Biomass Gasification and Pyrolysis: Practical Design and Theory. Academic Press, Elsevier, 2010.

21. Shudo T, Takahashi T, Influence of reformed gas composition on HCCI combustion engine system fueled with DME and H2eCOeCO2 which are onboard-reformed from methanol utilizing engine exhaust heat, Transactions of Japan Society of Mechanical Engineering, Part B 70 (698) (2004) 2663e2669.

22. Knoef HAM.. Handbook of Biomass Gasification. BTG, 2005.

23. Deshmukh SJ, Bhuyar LB and Thakre SB, 2008. Investigation on performance and emission characteristics of CI engine fuelled with producer gas and esters of Hingan (Balanites) oil in dual fuel mode. Int. J. Aerosp. Mech. Eng., Vol. 2.

24. Dasappa S, “On the estimation of power from a Diesel engine converted for gas operation a simple analysis” Tech. rep., ASTRA Indian Institute of Science, 2002.

25. Pedrazzi S, Allesina G, Morselli N, Puglia M, Leonardi C, Rinaldini CA, Savioli T, Mattarelli E, Giorgini L, Tartarini P. Modified diesel engine fueled by syngas: modeling and experimental validation. 24th European Biomass Conference and Exhibition, 6-9 June 2016, Amsterdam, The Netherlands.

26. Bibhuti B, Sahoo A, Niranjan Sahoo B, Ujjwal K. Saha B, Effect of H2:CO ratio in syngas on the performance of a dual fuel diesel engine operation, Applied Thermal Engineering 49 (2012) 139e146

27. Mahgoub BKM, Sulaiman SA and Abdul Karim ZA, 2013. Performance of a Compression Ignition Engine Fuelled by Diesel and Imitated Syngas. Asian Journal of Scientific Research, 6: 456-466. DOI:10.3923/ajsr.2013.456.466

28. Allesina G, Pedrazzi S, Montermini L, Giorgini L, Bortolani G, Tartarini, P Porous filtering media comparison through wet and dry sampling of fixed bed gasification products (2014) Journal of Physics: Conference Series, 547 (1), art. no. 012003

29. Allesina G, Pedrazzi S, Sgarbi F, Pompeo E, Roberti C, Vincenzo C, Tartarini P. Approaching sustainable development through energy management, the case of Fongo Tongo, Cameroon, International Journal of Energy and Enviromental Engineering, Volume 6, 2015, Pages 121-127.

30. UNI EN ISO 5167-1:2003 Measurement of fluid flow by means of pressure differential devices inserted in circular cross-section conduits running full -- Part 1: General principles and requirements

31. Cengel YA. Introduction to thermodynamics and heat transfer. McGraw-Hill, Boston 1997.

32. Wood Gas as an Engine Fuel, FAO (UN Food and Agriculture Organization) Forestry Division Publication 72, 1986 ISBN 92-5-102436-7

33 Fernandes FAN and Sousa EMM (2006), Fischer-Tropsch synthesis product grade optimization in a fluidized bed reactor. AIChE J., 52: 2844–2850. doi:10.1002/aic.10887

34 Rassweiler G, Withrow L. Motion pictures of engine flames correlated with pressure cards. SAE Paper 380139; 1938.